Hindawi
International Transactions on Electrical Energy Systems
Volume 2023, Article ID 2990504, 15 pages
https://doi.org/10.1155/2023/2990504

Research Article

A Sequential Generation Redispatch Algorithm to Ensure Power System Small Signal Stability under Low-Frequency Oscillations

Hassan Golzari-Kolur, Seyed Mohammad-Taghi Bathaee, and Turaj Amraee

K.N.Toosi University of Technology, Tehran, Iran

Correspondence should be addressed to Turaj Amraee; amraee@kntu.ac.ir

Received 18 November 2022; Revised 23 December 2022; Accepted 29 December 2022; Published 19 January 2023

Academic Editor: Mahdiyeh Eslami

Generation rescheduling is a major action against abnormal system conditions such as small signal instability. The operating point of the power system impacts the small signal stability; therefore, this article proposes a novel sequential generation rescheduling model as a preventive control against low-frequency fluctuations. An optimal power flow (OPF) problem is utilized to determine the base operating point. Then, in the process of improving the small signal stability, the modal analysis specifies the system stability status in each step, and the proposed second-order convex redispatch model defines the optimal direction of generation rescheduling. Small signal stability is considered a constraint in this model. Using a sensitivity analysis, system generators and system buses are divided into two increasing and decreasing groups, which are included in the model according to their contribution coefficients in damping improvement. Finally, the alternating current (AC) power flow analysis provides the subsequent operating points. The redispatch model is solved using the quadratic programming algorithm, and the Newton algorithm is used to manage the nonlinear and nonconvex characteristics of the power flow model. The proposed method is simulated over the IEEE 9, 39, and 118 bus test systems. It is shown that the proposed method increases the damping of the power system from the unstable state to the desired condition by controlling the operating point.

1. Introduction

Small signal stability is critical to the security and stability of the power system. The expansion of interconnected power systems and economic constraints has forced utilities to operate their own systems close to the stability boundaries. In such a situation, the sudden changes in power balance such as load insertion and removal or other contingencies such as line outages will cause low-frequency oscillations. Also, the rise of renewable energy sources such as wind and solar farms makes the situations more complex. Therefore, the damping of critical modes should be improved to secure system operation and ensure system small signal stability. To this end, many reported studies have shown the importance and effectiveness of the damping controllers. The enhancement of system small signal stability has been tackled by using power oscillation damping controllers installed at flexible AC transmission system (FACTS) devices [1, 2], installing power system stabilizer (PSS) on generators [3–5], adding control loops on HVDC [6], and so on. Although these damping controllers are effective, there are reasons that confirm they are not the best strategy and cannot guarantee the small signal stability at all times. Conventional damping controllers require a long process of design, construction, and installation; they need complete technical specifications of the system, and there are always operating conditions different from what the controllers are designed for [7]. At the operational level, the rescheduling of generating units, taking into account the stability criteria, can provide a corrective measure to ensure the small-signal stability of a power system. The latter method has received a lot of attention in recent years because it provides an appropriate level of security for the power system by considering economic objectives and technical constraints.

Generation redispatch can be done using either a data-driven or a model-driven method. In the area of data-based

techniques, an online preventative control strategy is proposed in [8] that takes transient stability into consideration. Using a decision tree, the power system stability is assessed; the derived rules are then incorporated to the conventional optimal power flow. In [9], classification tree is used to formulate small signal stability as a constraint in the optimal power flow. As an extension of this work, [10] proposes an AC security-constrained OPF method instead of DC security-constrained OPF that provides $N-1$ security and small-signal stability. Reference [11] uses a neural network to convert the feasible space of the nonlinear AC security-constrained OPF problem into a mixed integer linear model to make it computationally tractable. The authors in [12] introduced a new approach using LQ-decomposition-based recursive sub-DMD to identify the relationships between generators power and system modes. Then, a redispatch strategy supported by the participation factor is suggested to improve the damping ratio of the power system.

The available model-driven generation rescheduling methods are time consuming due to the high computational complexity. In [7], the numerical sensitivities of eigenvalue with respect to active power of generating units have been calculated to select the generators to be rescheduled for improving the power transfer capability. In [13], an optimal preventive control strategy is proposed by including small signal stability constraints in the optimal power flow (OPF), which ensures an appropriate level of security under stressed loading conditions. Since the small signal stability constraint is nonlinear and nonsmooth, the stability and sensitivity analysis are valid only at the initial operating point. Therefore, the proposed methods cannot guarantee the convergence of the optimization problem. The closed-form eigenvalue sensitivity method [14, 15] is used to include the small signal stability constraint in expected-security-cost optimal power flow [16]. To implement the primal-dual interior-point algorithm, first and second-order sensitivity is necessary, which makes the proposed method very time-consuming. Small signal stability constrained-optimal power flow (SSSC-OPF) is addressed as an Eigenvalue optimization problem in [17]. Based on Lyapunov's stability theorem, a nonlinear semidefinite programming (NLSDP) model and algorithm are proposed. Because of the particular characteristics of this method, like dense matrix variables, it cannot be applied to large-scale power systems. In the generation rescheduling algorithm proposed by [18], the critical generators are identified using the normalized participation factor so that under a stress power system condition, the small signal stability is guaranteed and the available transmission capability is maintained. Regarding the preservation of the network model, a new approach for calculating analytical eigenvalue sensitivities according to different operating parameters has been proposed in [19]. Using the proposed method, the most effective generators are selected to suppress the low-frequency oscillations. In [20], the minimum redispatch to increase the damping coefficient is determined using numerically-calculated generation sensitivities. In [21], a convexification approach is proposed to resolve the small signal stability-constrained OPF problem without the need for linearization of power system equations and eigenvalue analysis. In [22], a stability criterion is defined based on the energy of interarea oscillations, which is then included in the optimal power flow problem to investigate the effect of the operating point on the dynamics of power grids. In order to make the SSSC-OPF formulation computationally tractable, it is convexified using SDP relaxation techniques.

As the operating conditions change, the eigenvalues of the system change. Therefore, this local validity should be considered in the retuning of generator setpoints. To address this issue, various sequential methods have been used but with a high computational burden. In [23], a sequential quadratic programming method combined with gradient sampling is proposed to deal with the nonsmooth property of the spectral abscissa function. To improve the convergence of SSSC-OPF, authors in [24] propose a sequential programming method that decomposes the main problem into a sequence of subproblems. Since each subproblem consists of two nonlinear optimization problems, and this method is computationally complex and time consuming.

In this paper, in order to deal with the discontinuity nature of the small signal stability index, a sequential solution approach is adopted, and also to reduce the computational burden and complexity, a second-order convex power generation rescheduling model is proposed. First, the OPF model is solved with the aim of minimizing the production cost of the generators. Power balance equations, branch flow limits as well as upper and lower limits of generation levels and voltage limits are considered as constraints. The results are used to extract a state-space model of the power system and calculate system eigenvalues. In case of instability or undesirable damping ratio, the generators are dispatched to provide the specified conditions. Critical eigenvalues are identified at each step to manage their cyclical behaviour. Also, to ensure the effectiveness of the small signal stability index linearization, the amount of change in the active power of the generators and the bus voltage magnitudes is limited.

The rest of this paper is organized as follows: Section 2 is dedicated to the problem formulation. Small signal stability and OPF problem are briefly introduced and modelled in Sections 2.1 and 2.2, respectively. In Section 3, the modelling of the proposed method is described. Section 4 evaluates the effectiveness of the proposed method by applying it to three different test systems. Section 5 concludes the article.

2. Problem Formolation

Change of system operating conditions affects the stability and economic efficiency of the power system, so to achieve various objectives of generation scheduling, security and economic indices need to be taken into account in dispatch strategies. The purpose of this section is to consider the small signal stability in economic generation dispatch or OPF problem.

2.1. Optimal Power Flow. In the proposed method, the base operating conditions are determined by solving the OPF model. Standard OPF as a constrained optimization problem consists of an objective function with a set of equality and inequality constraints. The standard form of the OPF problem is as follows [25]:

$$\min_{\mathbf{y}} \mathbf{f}(\mathbf{y}), \tag{1}$$

$$\mathbf{g}(\mathbf{y}) = 0, \tag{2}$$

$$\mathbf{h}(\mathbf{y}) \leq 0, \tag{3}$$

$$\mathbf{y_{min}} \leq \mathbf{y} \leq \mathbf{y_{min}}. \tag{4}$$

Equation (1) is the objective function, which is considered a quadratic function of the output power of generators. The equality constraints are represented by (2) that are conventionally defined as nodal power balance equations. The set of inequality constraints including the branch flow limits are represented by (3) and is the optimization variable, which includes the active/reactive powers and bus voltage phasors.

2.2. Small Signal Stability. Small signal stability refers to the ability of the power system to maintain synchronism under small disturbances such as load perturbation [26]. To study the small signal stability, the dynamic behaviour of power systems is described by a set of differential and algebraic equations (DAE) [27]. Generator dynamics as differential equations and the network model as the algebraic equations can be written in the following compact form:

$$\begin{aligned} \dot{\mathbf{x}} &= \mathbf{j}_1(\mathbf{x}, \mathbf{z}, \mathbf{d}), \\ 0 &= \mathbf{j}_2(\mathbf{x}, \mathbf{z}), \end{aligned} \tag{5}$$

where $\mathbf{x}$ and $\mathbf{z}$ are vectors of system state and algebraic variables, respectively, and $\mathbf{d}$ is the input to the system. The power system model is nonlinear, but it can be linearized at a specific operating point to analyse the small signal stability. The first-order approximation of the Taylor series of the power system equations around the equilibrium point leads to the following equation:

$$\begin{bmatrix} \Delta\dot{\mathbf{x}} \\ 0 \end{bmatrix} = \begin{bmatrix} \mathbf{A} & \mathbf{B} \\ \mathbf{C} & \mathbf{D} \end{bmatrix} \begin{bmatrix} \Delta\mathbf{x} \\ \Delta\mathbf{z} \end{bmatrix} + \begin{bmatrix} \mathbf{E} \\ 0 \end{bmatrix} \Delta\mathbf{d}. \tag{6}$$

Assuming $\mathbf{D}$ as a nonsingular matrix, $\Delta\mathbf{z}$ can be removed from the set of equations, and we can achieve the following:

$$\begin{aligned} \Delta\mathbf{z} &= -\mathbf{D}^{-1}\mathbf{C}\Delta\mathbf{x}, \\ \Delta\dot{\mathbf{x}} &= \mathbf{A_s}\Delta\mathbf{x} + \mathbf{E}\Delta\mathbf{d}, \\ \mathbf{A_s} &= \mathbf{A} - \mathbf{B}\mathbf{D}^{-1}\mathbf{C}, \end{aligned} \tag{7}$$

where $\mathbf{A_s}$ is known as the system state matrix. Once the system state matrix is specified, the stability condition of the linear system can be determined from the eigenvalue problem:

$$\begin{aligned} A_s\mathbf{v} &= \lambda\mathbf{v}, \\ A_s^T\mathbf{u} &= \lambda^T\mathbf{u}, \end{aligned} \tag{8}$$

where $\mathbf{u}$ and $\mathbf{v}$ are matrices of the left and right eigenvectors, respectively, and λ is a diagonal matrix of eigenvalues. According to Lyapunov theory, the system is stable in terms of small signal stability if the real part of all eigenvalues of the state matrix is nonpositive. In this article, the minimum damping ratio of the system is considered as a small signal stability index:

$$\xi = \frac{-\alpha}{\sqrt{\alpha^2 + \beta^2}}, \quad \lambda = \alpha + \beta i, \tag{9}$$

$$\xi_{\min} = \min\{\xi(\lambda) \colon \lambda \epsilon \boldsymbol{\lambda}(\mathbf{A}_s)\}. \tag{10}$$

The stability index is considered as and for the unstable $\xi_{\min} \geq 0$ and $\xi_{\min} \geq \xi_{DDR}$ stable system, respectively. ξ_{DDR} is the predetermined desired damping ratio (DDR).

3. Modeling the Proposed Method

Since the small signal stability is evaluated after the linearization of the power system equations around a particular operating point, the direct solution of the optimization problem that creates a different operating point does not preserve the small signal stability analysis. As shown in Figure 1, we deal with this issue using a sequential approach. Using the standard OPF that takes into account the AC power flow, the initial operating point is determined and the subsequent operating points are determined based on the power flow. In solving the power flow problem, two known quantities associated with each bus should be determined. Since the amount of network load does not change during the stability improvement process, the load demand (P-Q) is known. In the case of regulated or voltage-controlled buses (PV buses), the active power and voltage magnitude are obtained by solving the redispatch model.

3.1. Redispatch Problem

3.1.1. The Objective Function. The objective function is defined as the total production cost of generation redispatch of generators as given in the following equation:

$$f = \sum_{i \epsilon \mathbb{N}G} c_i \Delta P_{Gi}^2, \tag{11}$$

where ΔP_{Gi} is the change of output powers of the generators and c_i is the coefficient of the cost function of the generators. In this article, for the sake of simplicity, the cost of all generators is assumed as $c = 1$, and therefore, the objective is to minimize changes in the output power of the generators. Without loss of generality, any other cost vector can be assumed.

3.1.2. Generation Redispatch Constraint. In the generation rescheduling process, in order to maintain the total active

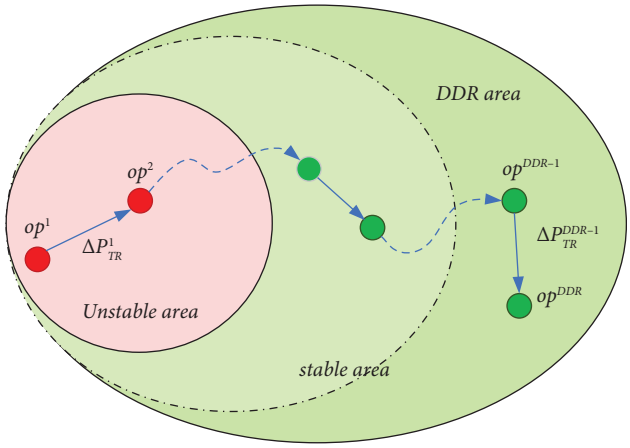

Figure 1: Picture of the proposed sequential method.

power of the system, power balance without losses is considered as

$$\sum_{i \epsilon \mathbb{N}_G} \Delta P_{Gi} = 0. \tag{12}$$

In each step, alternating current (AC) power flow is used to determine the operating point, which takes losses into account. However, for moving from one operating point to another point and determining the direction of redispatch, because the losses of the transmission system are insignificant and on the contrary, redispatch does not create a noticeable change in the losses, so it is ignored.

3.1.3. Small Signal Stability Constrain. In order to move towards the stability region or improve the damping ratio of the system, the damping should be increased in each step. If y is an optimization variable, using the Taylor expansion of the damping ratio, we have the following:

$$\xi(y_0 + \Delta y) \geq \xi(y_0) + \frac{\partial \xi}{\partial y} \Delta y, \tag{13}$$

where $(\partial \xi / \partial y)$ is the first-order sensitivity of the damping ratio. To determine the status of the voltage-controlled buses at the new operating point, the active power of the generators and the voltage magnitude of the buses are considered as optimization variables. Therefore, the sensitivity of the damping ratio to these two variables is determined, and the small signal stability constraint is considered according to (14) in the optimization problem as follows:

$$\sum_{i \epsilon \mathbb{N}_G} \frac{d\xi}{dP_{Gi}} \Delta P_{Gi} + \sum_{m \epsilon \mathbb{N}_B} \frac{d\xi}{dV_m} \quad \Delta V_m \geq \Delta \xi. \tag{14}$$

Voltage magnitude of a given bus at the beginning of each subsequence is V_k^0, and the regulation of the bus voltage is defined as $\Delta V_k = \Delta V_k - V_k^0$. To calculate the sensitivity of the stability index, the closed-form analytical formula has been used [18]. In this method, the sensitivity of an eigenvalue to the optimization variable is calculated by the following equation:

$$\frac{\mathrm{d}\lambda}{\mathrm{d}x} = \frac{u^T \mathrm{d}A_s / \mathrm{d}x v}{u^T v}. \tag{15}$$

Utilizing (9) and (15), the first-order sensitivity of the damping ratio is evaluated as

$$\frac{\mathrm{d}\xi}{\mathrm{d}x} = \frac{-\beta^2}{\sqrt[3]{\alpha^2 + \beta^2}} \frac{\mathrm{d}\alpha}{\mathrm{d}x} + \frac{\alpha\beta}{\sqrt[3]{\alpha^2 + \beta^2}} \frac{\mathrm{d}\beta}{\mathrm{d}x}. \tag{16}$$

In problem modelling, the damping ratio is defined as a hard constraint, while the operating cost is included in the model as a soft constraint or objective function, so it can be concluded that the desired damping is provided with the lowest cost.

3.1.4. Redispatch Limits. At the beginning of each subsequence, the sensitivity of the damping ratio with respect to the active power of the generators is calculated, and according to their algebraic sign, the generators are classified into two groups, namely, increasable generators (IG) and decreasable generators (DG) [28]. Generators with a larger sensitivity magnitude have a greater effect on improving system damping. The effect of generators in each group can be determined through their contribution coefficient as follows:

$$\begin{aligned} cc_i^{IG} &= \frac{\mathrm{d}\xi / \mathrm{d}P_i}{\sum_{j \epsilon \mathbb{N}_{IG}} \mathrm{d}\xi / \mathrm{d}P_j}, \quad i \epsilon \mathbb{N}_{IG}, \\ cc_i^{DG} &= \frac{\mathrm{d}\xi / \mathrm{d}P_i}{\sum_{j \epsilon \mathbb{N}_{DG}} \mathrm{d}\xi / \mathrm{d}P_j}, \quad i \epsilon \mathbb{N}_{DG}, \end{aligned} \tag{17}$$

where $\mathbb{N}_{IG}$ and $\mathbb{N}_{DG}$ are sets of increasing (generators that should increase their power) and decreasing generators, respectively. The maximum power transfer from the decreasing group is determined by their total power reserve (14), and then, by a factor of w, the amount of power that must be transferred from the decreasing to the increasing group is determined as follows:

$$P_{TR}^{DG} = \sum_{i \epsilon \mathbb{N}_{DG}} P_{Gi} - P_{Gi}^{\min}, \tag{18}$$

$$\Delta P_{TR} = w * P_{TR}^{DG}. \tag{19}$$

On the one hand, to increase the effectiveness of stability index calculation, the amount of power exchange between the two groups in each subsequence should not be considered too large. On the other hand, if the amount of power exchange is considered small, the number of subsequence's increases, resulting in a high computation time. The determined power should be distributed or dispatched among the generators of each group by the contribution coefficient as follows:

$$\begin{aligned} \Delta P_i^{IG} &= cc_i^{IG} * \Delta P_{TR}, \\ \Delta P_i^{DG} &= cc_i^{DG} * \Delta P_{TR}. \end{aligned} \tag{20}$$

Since there must be a balance between power redistribution, the maximum reserve available in the IG group, P_{TR}^{IG}, given by (21), must be greater than the determined power ΔP_{TR}:

$$P_{TR}^{IG} = \sum_{i\epsilon \mathbb{N}IG} P_{Gi}^{\max} - P_{Gi}. \tag{21}$$

After determining the contribution of each generator to the determined power exchange, the limits of power changes in the form of (22) are added to the problem model:

$$0 \le \operatorname{sign}\left(\frac{\mathrm{d}\xi}{\mathrm{d}P_G}\right) * \Delta \mathbf{P}_G \le \boldsymbol{\gamma}, \boldsymbol{\gamma} = \left\{\Delta \mathbf{P}^{IG} \Delta \mathbf{P}^{DG}\right\}. \tag{22}$$

3.1.5. Voltage Change Limits. The algebraic sign of the system damping ratio sensitivity with respect to the bus voltage magnitude is used to divide the system buses into two groups of increasable buses (IB) and decreasable buses (DB). Then, the impact of the buses in each group is determined by their contribution coefficients as follows:

$$\begin{aligned} cc_k^{IB} &= \frac{\mathrm{d}\xi/\mathrm{d}V_k}{\sum_{j\epsilon \mathbb{N}_{IB}} \mathrm{d}\xi/\mathrm{d}V_j}, \quad k \epsilon \mathbb{N}_{IB}, \\ cc_k^{DB} &= \frac{\mathrm{d}\xi/\mathrm{d}V_k}{\sum_{j\epsilon \mathbb{N}_{DB}} \mathrm{d}\xi/\mathrm{d}V_j}, \quad k \epsilon \mathbb{N}_{DB}, \end{aligned} \tag{23}$$

where $\mathbb{N}_{IB}$ and $\mathbb{N}_{DB}$ are sets of increasable and decreasable buses, respectively. Using the contribution coefficients of buses, the limits of voltage magnitude changes, according to (25), are added to the proposed model.

$$\Delta \mathbf{V}_{\mathrm{IB}} = \mathbf{cc}^{\mathrm{IB}}, \tag{24}$$

$$\Delta \mathbf{V}_{\mathrm{IB}} = \mathbf{cc}^{\mathrm{DB}}, \tag{25}$$

$$\begin{aligned} &0 \le \operatorname{sign}\left(\frac{\mathrm{d}\xi}{\mathrm{d}V}\right) * \mathbf{V} \le \boldsymbol{\rho}, \\ &\boldsymbol{\rho} = \left\{\Delta \mathbf{V}_{\mathrm{IB}} \Delta \mathbf{V}_{\mathrm{DB}}\right\}. \end{aligned} \tag{26}$$

Therefore, the optimization problem can be summarized as follows:

$$\begin{aligned} &\min f = \sum_{i\epsilon \mathcal{S}G} c_i \Delta P_{Gi}^2, \\ &s.t. \sum_{i\epsilon \mathcal{S}_G} \Delta P_{Gi} = 0, \sum_{i\epsilon \mathbb{N}_G} \frac{\mathrm{d}\xi}{\mathrm{d}P_{Gi}} \Delta P_{Gi} + \sum_{k\epsilon \mathbb{N}_B} \frac{\mathrm{d}\xi}{\mathrm{d}V_k} \Delta V_k \ge \Delta\xi, 0 \le \operatorname{sign}\left(\frac{\mathrm{d}\xi}{\mathrm{d}P_G}\right) * \Delta P_G \le \gamma, 0 \le \operatorname{sign}\left(\frac{\mathrm{d}\xi}{\mathrm{d}V}\right) * V \le \rho. \end{aligned} \tag{27}$$

3.2. Power Flow Analysis. At the third step, an AC power flow model is conducted to determine the new operating point. Considering the generators as power sources and based on the admittance matrix, the AC power flow equations are expressed as a set of nonlinear algebraic equations as given as follows:

$$P_{Gj} - P_{Lj} = \sum_{K\epsilon \mathbb{N}_B} V_j V_k Y_{ik} \cos\left(\theta_j - \theta_k - \phi_{ik}\right), \quad (\text{for } j \epsilon \mathbb{N}_B), \tag{28}$$

$$Q_{Gj} - Q_{Lj} = \sum_{K\epsilon \mathbb{N}_B} V_j V_k Y_{ik} \sin\left(\theta_j - \theta_k - \phi_{ik}\right), \quad (\text{for } j \epsilon \mathbb{N}_B). \tag{29}$$

To solve the power flow problem, there are several types of iterative methods, often based on the Newton method or the Gauss–Seidel method. Due to quadratic convergence and high accuracy, we use the Newton–Raphson algorithm in the proposed method.

3.3. Proposed Sequential Method. In the first step of the proposed method, the OPF problem is solved, and the initial operating point of the system is obtained. Modal analysis then determines the small signal stability of the power system. If the system is unstable or the damping ratio is not desirable, the next operating point is obtained through power flow. This process of analysing stability and power flow continues until the desired operating point is reached. The proposed method uses a convex optimization model, which provides a global solution. It should also be noted that during the steps, system generators and system busses are divided into increasing and decreasing groups using modal analysis and sensitivity, and on the other hand, the system damping ratio trend is increasing and has few changes. Therefore, it can be concluded that the proposed method converges. The accuracy of this issue has been confirmed in the simulations. The pseudocode for the proposed method is illustrated in Algorithm 1. It is worth noting that the redispatch as an emergency action is done for a time step in the near future, for example, for the next hour. However, without losing the generality of the problem, it can be done for a fraction of the next hour or several hours.

Input:
$y^{(0)}$ = Initial operating condition from conventional OPF
ξ_{DDR}: Desirable SSS level
w: Power rescheduling coefficient
(1) Execute small signal stability analysis at $y^{(0)}$
(2) $m \longleftarrow 1, \xi \longleftarrow \xi(y^{(0)})$
(3) **while** $\xi < \xi_{DDR}$
(4) Use the sensitivities $d\xi/dP_G$ to determine $\Delta\mathbf{P}^{IG}$ and $\Delta\mathbf{P}^{DG}$
(5) Use the sensitivities $d\xi/dV$ to determine $\Delta\mathbf{V}_{IB}$ and $\Delta\mathbf{V}_{DB}$
(6) Solve optimization problem given in (27)
(7) $y^{(m)} \longleftarrow$ solve power flow equation given in (28)-(29)
(8) Execute small signal stability analysis at $y^{(m)}$
(9) $m \longleftarrow m + 1, \xi \longleftarrow \xi(y^{(m)})$
(10) **end while**
Output:
$y^{(m)}$: desired operating point from proposed method

Algorithm 1: Proposed sequential method.

4. Numerical Simulation

In this section, the effectiveness of the proposed methodology is evaluated by three different IEEE test systems. Modal analysis at the base operating point shows that the first two systems (small and medium scale) are stable, but the third system is unstable. Therefore, by applying the proposed method, we are looking for the test to increase the damping to the optimal level and the stabilization test, which is an excellent benchmark to measure its validity. MATLAB software is used to solve the optimization problem and perform the modal analysis. In all test systems, the two-axis model is used to represent the generator and the excitation system is modelled by IEEE Type I [27]. The related equations are summarized in Appendix.

4.1. IEEE 9-Bus System. The 9-bus system has 3 generators and has been used in various studies for small signal stability analysis. The steady-state and dynamic data of this system are extracted from [29, 30], respectively. At the initial operating point of this system, OPF and modal analysis are performed, and the damping ratio of the system at base case is 2.1%. Since the system is stable, we applied the proposed method to increase the system damping ratio to 5%; the results are given in Table 1. The system modes are sorted in column 4 based on the system damping (from low to high damping) and in column 5 based on the magnitude of the real part, which are the same in this particular case. It can be seen that to achieve the 5% damping ratio, the generation of unit 1 is increased from 89.8 MW at base case to 141.3 MA at Case 2. At the same time, both G2 and G3 reduce their generation levels to 89.5 MW and 85.7 MW, respectively.

The trace of two modes of the system with the lowest damping ratio along with the path of increasing their damping ratio during the process of applying the proposed method is shown in Figure 2. It is observed that the proposed method has increased the damping ratio of these two modes from 2.1% to 5% and from 3.7% to 5.5%, respectively, and provides an appropriate damping for the system.

4.2. IEEE 39-Bus System. The 39-bus system has 10 generators, and the steady-state and dynamic data of this system are provided in [28, 31], respectively. The damping ratio of the system at the initial operating point is 2.5%. To ensure the small signal stability, we implemented the proposed method with a damping ratio threshold of 5%. Critical eigenvalues with damping ratios less than 5% under different operating conditions are provided in Table 2. As can be seen from Table 2, eigenvalues exhibit a cyclic behaviour at different operating points. For example, the fifth mode at the initial operating point changes to the seventh and critical mode of the system at points with damping ratios of 4% and 5%, respectively. Therefore, it can be concluded that sequential methods are more effective for redistribution of power generation.

Using modal analysis, the sensitivity of critical eigenvalue with respect to output power, contribution coefficient and power change of generators at different operating points are shown in Figures 3–5, respectively. As it can be deduced from the figures, for example in operation point 3, increasing the output of generator 8 and reducing the generation of unit 3 have the greatest effect on improving the system damping.

For six different operating points, Figure 6 shows the trace of improving the damping ratio of eight system modes that have a damping ratio of less than 5% at the base operating point. As a result, the proposed method has been successful in improving the stability of the system and has provided an opportunity to select different operating points at different times. Additionally, Figure 7 shows the path of the minimum damping ratio of the system as a result of using the proposed method.

In order to investigate the completely nonlinear behaviour of the power system, we use time-domain simulation because the small signal stability analysis is

Table 1: Results of the proposed method for IEEE 9-bus system.

OP	Generation, Cost	Damping, Ratio (DR : %)	Lambda, min DR	Lambda, max real part	P_{G1}	P_{G2}	P_{G3}	$V_1\,(pu)$	$V_2\,(pu)$	$V_3\,(pu)$
Base case	5303.7	2.1	$-0.17 \pm 8.18i$	$-0.17 \pm 8.18i$	89.8	134.4	94.2	1.04	1.095	1.078
Case 1	5510.8	4	$-0.31 \pm 7.91i$	$-0.31 \pm 7.91i$	126.2	104.4	85.8	1.04	1.094	1.075
Case 2	5769.6	5	$-0.39 \pm 7.80i$	$-0.39 \pm 7.80i$	141.3	89.5	85.7	1.04	1.094	1.074

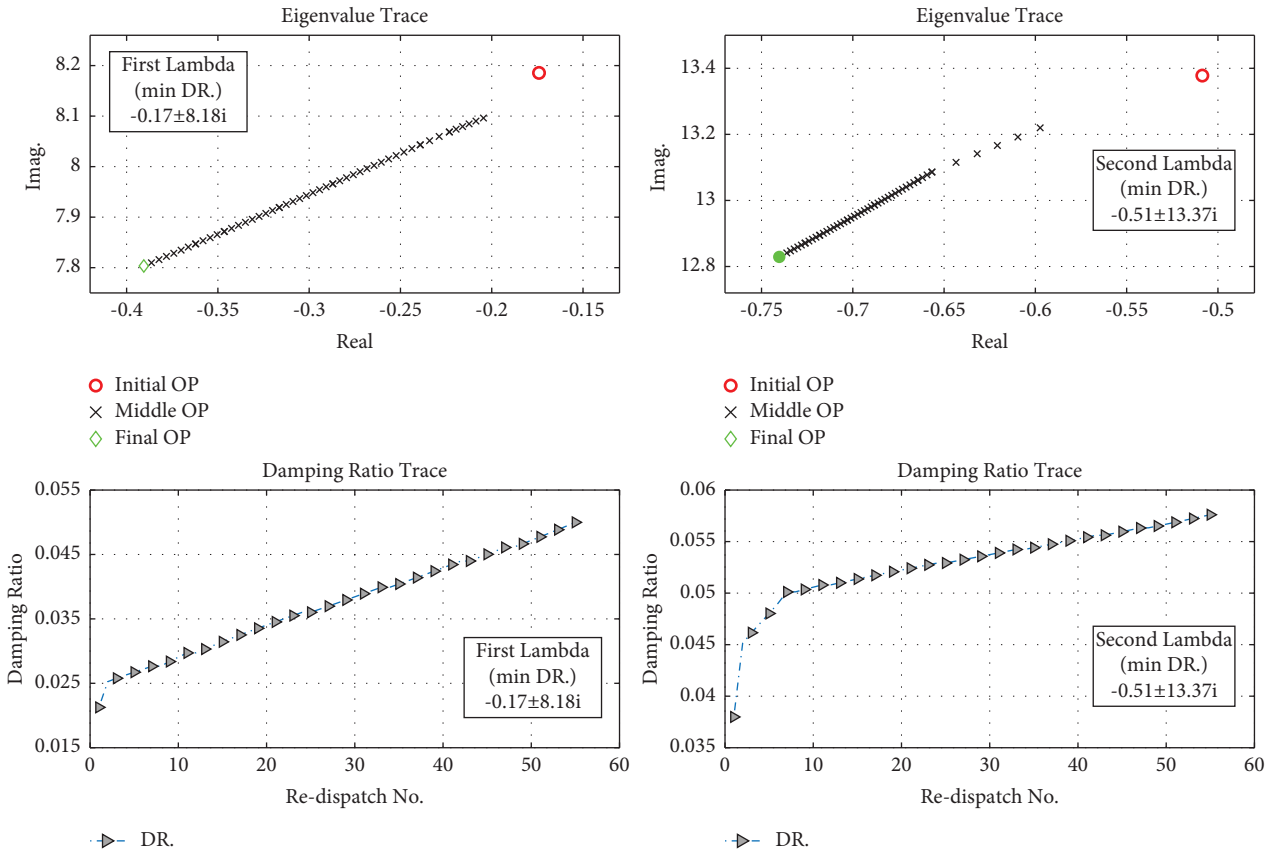

Figure 2: The trace of two modes with the lowest damping ratio and their damping ratio.

Table 2: Critical modes and their damping ratios under different operating points for IEEE 39-bus system.

Mode no.	Mode	Damping ratio
DR. (2.5~5) %		
1	$-0.20 \pm 7.92i$	0.0250
2	$-0.20 \pm 6.57i$	0.0308
3	$-0.28 \pm 8.65i$	0.0318
4	$-0.23 \pm 7.04i$	0.0330
5	$-0.26 \pm 6.08i$	0.0425
6	$-0.38 \pm 8.93i$	0.0432
7	$-0.37 \pm 8.15i$	0.0455
8	$-0.20 \pm 4.00i$	0.0490
DR. (3~5) %		
2	$-0.20 \pm 6.52i$	0.0301
1	$-0.24 \pm 7.91i$	0.0303
3	$-0.27 \pm 8.64i$	0.0316
4	$-0.23 \pm 6.98i$	0.0339
7	$-0.34 \pm 8.14i$	0.0412

Table 2: Continued.

Mode no.	Mode	Damping ratio
5	−0.26 ± 6.06i	0.0422
6	−0.38 ± 8.91i	0.0425
8	−0.20 ± 3.98i	0.0496
DR. (3.5~5) %		
7	−0.29 ± 8.13i	0.0351
4	−0.24 ± 6.94i	0.0353
6	−0.31 ± 8.78i	0.0358
5	−0.22 ± 6.08i	0.0358
1	−0.29 ± 7.93i	0.0361
2	−0.24 ± 6.53i	0.0362
3	−0.32 ± 8.67i	0.0370
8	−0.19 ± 3.99i	0.0487
DR. (4~5) %		
2	−0.24 ± 6.07i	0.0401
1	−0.31 ± 7.62i	0.0402
3	−0.34 ± 8.32i	0.0406
4	−0.27 ± 6.58i	0.0409
6	−0.35 ± 8.55i	0.0410
7	−0.33 ± 7.92i	0.0411
5	−0.22 ± 5.36i	0.0419
—	−0.24 ± 3.65i	0.0657
DR. (4.5~5) %		
2	−0.26 ± 5.81i	0.0453
7	−0.36 ± 7.79i	0.0460
4	−0.29 ± 6.34i	0.0463
6	−0.38 ± 8.22i	0.0467
1	−0.35 ± 7.49i	0.0468
5	−0.25 ± 5.05i	0.0498
3	−0.63 ± 7.99i	0.0786
—	−0.86 ± 9.69i	0.0888
DR. (5~. . .) %		
5	−0.25 ± 5.03i	0.0497
1	−0.37 ± 7.38i	0.0499
4	−0.28 ± 5.69i	0.0500
6	−0.42 ± 8.19i	0.0513
7	−0.39 ± 7.46i	0.0524
3	−0.46 ± 8.04i	0.0570
2	−0.41 ± 6.09i	0.0673
—	−0.88 ± 9.48i	0.0870

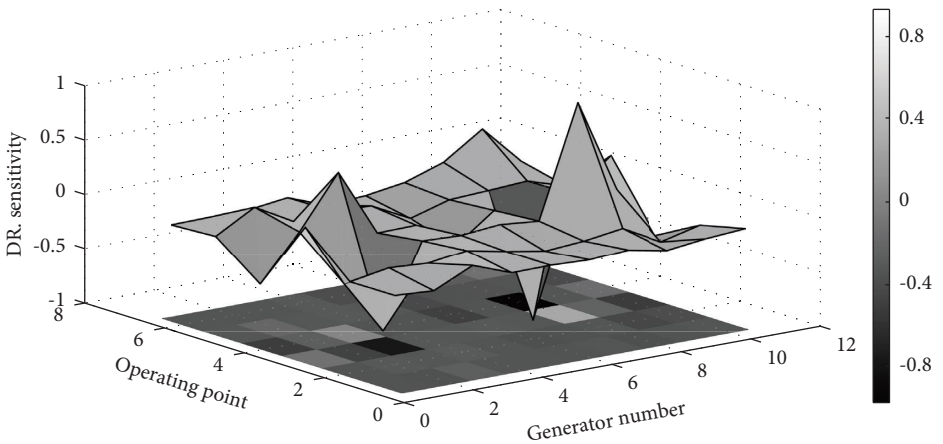

Figure 3: Damping ratio sensitivity at different operating points for IEEE 39-bus system.

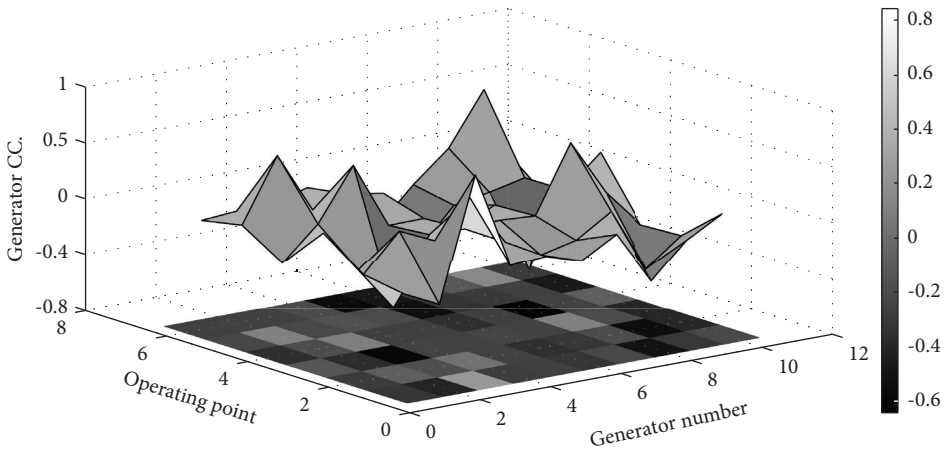

Figure 4: Generator contribution coefficient at different operating points for IEEE 39-bus system.

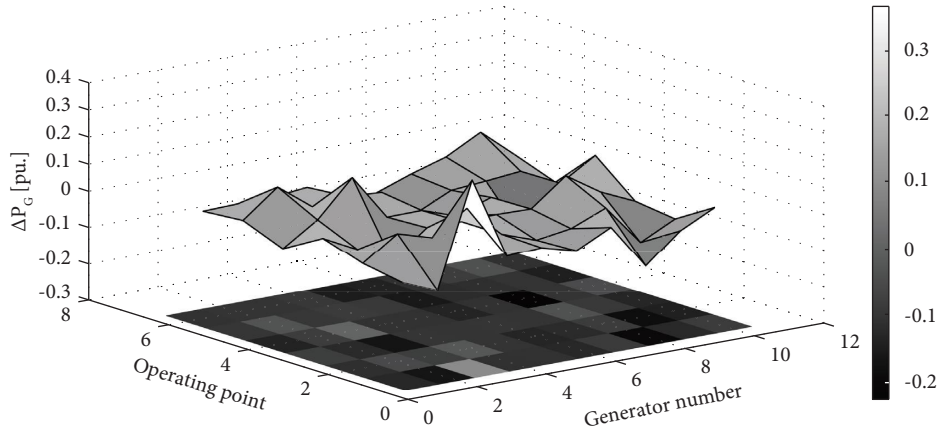

Figure 5: Generator power change limits at different operating points for IEEE 39-bus system.

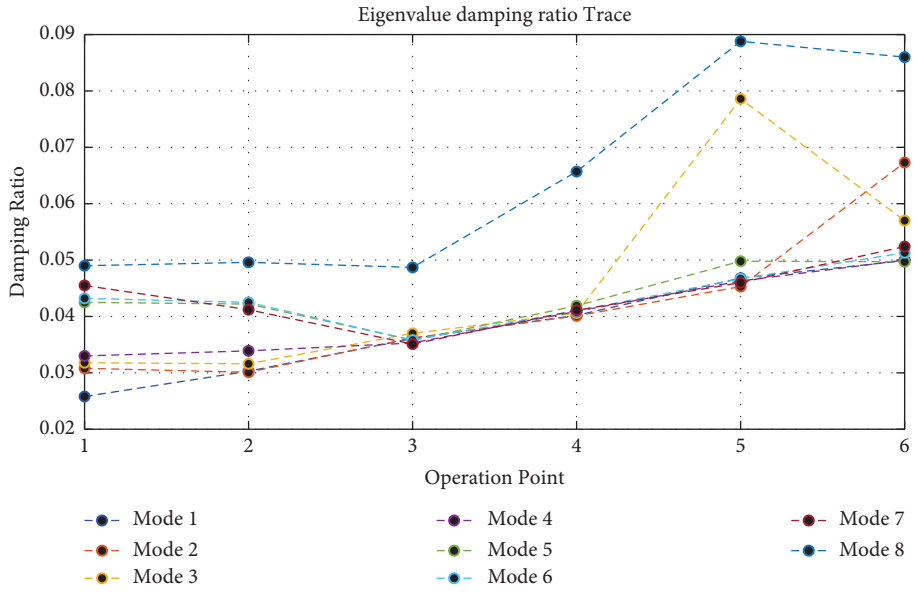

Figure 6: Damping ratio of critical modes of the system at different operating points for IEEE 39-bus system.

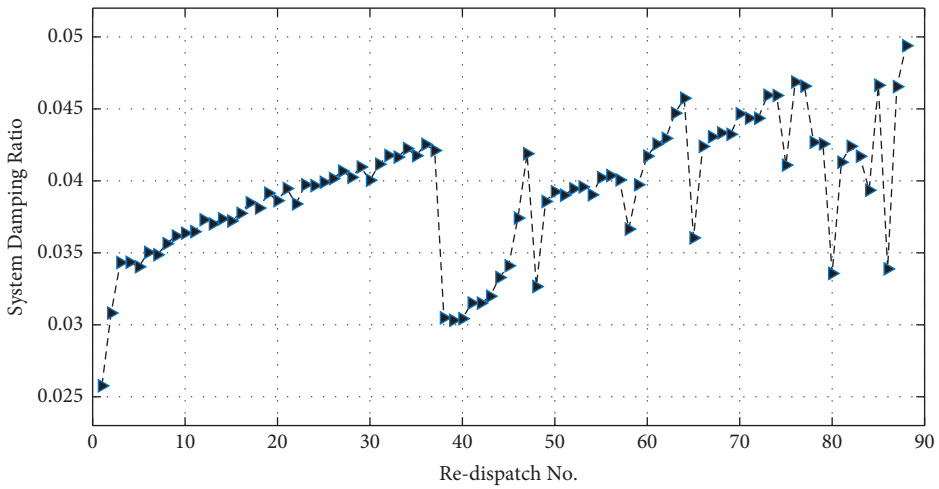

Figure 7: Trace of system damping ratio for IEEE 39-bus system.

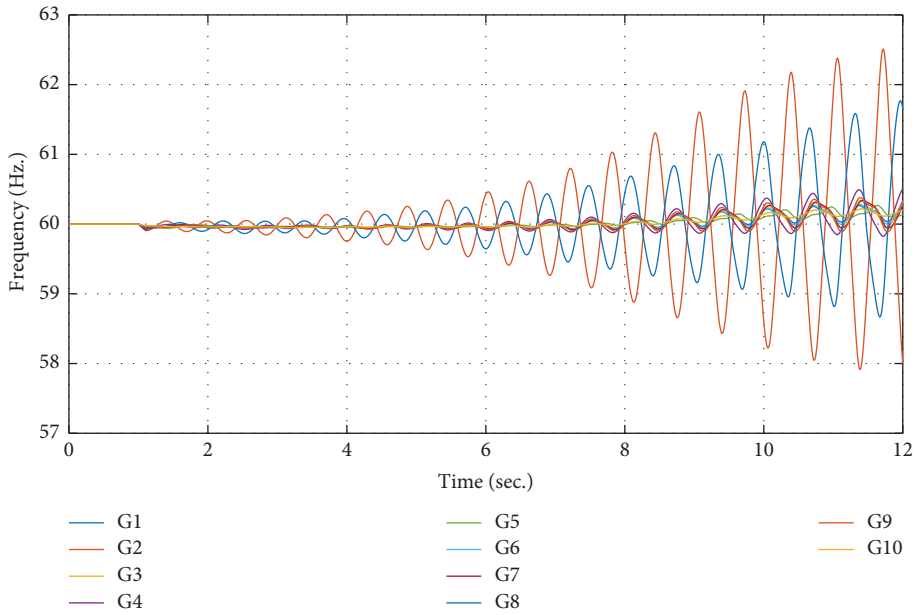

Figure 8: Time-domain simulation of IEEE 39-bus system for conventional OPF.

performed by means of a linear model of the power system. By considering the nonlinear differential algebraic model and increasing the system load by 20% as a disturbance, simulation has been performed for the operating conditions obtained from the conventional OPF and the proposed method. This analysis is a type of time domain electro-mechanical simulation and not a time domain electro-magnetic simulation. Therefore, under small disturbances, the small signal instability shows itself in the form of low-frequency oscillations. The frequencies of all generators for two methods are shown in Figures 8 and 9. As can be seen, the proposed method dampens the oscillations, and as a result, the system remains stable, while under conventional OPF, the system becomes unstable.

4.2.1. Comparative Analysis. The following three comparison cases are considered in order to evaluate the effectiveness of the proposed method:

(i) BCO: the basic conventional OPF that determines initial operating point without small signal stability limits

(ii) SSO: small signal stability-constrained OPF, which considers only the critical eigenvalue of the initial operating point [17]

(iii) PSM: proposed sequential method

According to the simulation, the IEEE 39-bus system is stable at the initial operating point. To investigate unstable conditions, we increase the system load by 10% and consider a contingency in the form of a single line outage (between

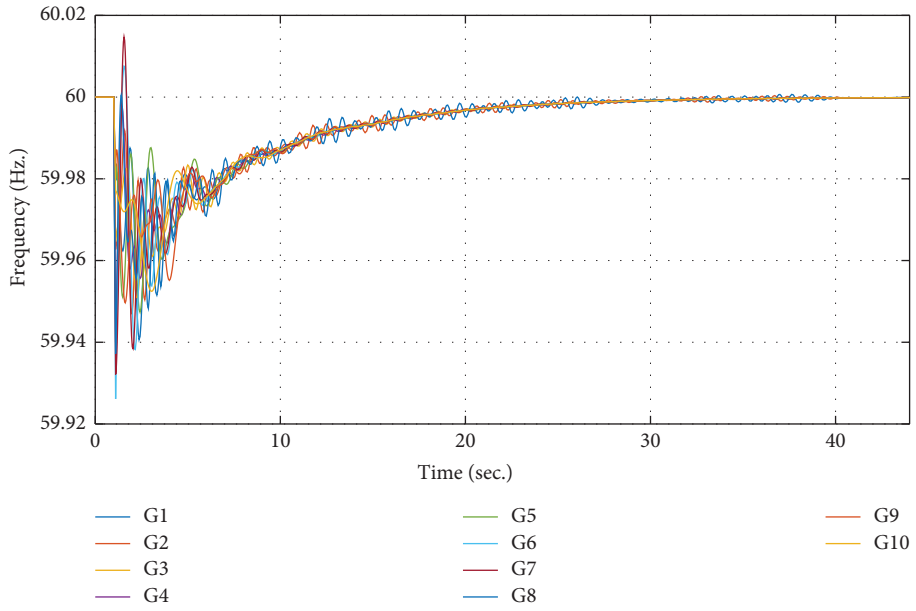

Figure 9: Time-domain simulation of IEEE 39-bus system for the proposed method.

Table 3: Comparing performance of three methods in the IEEE 39-bus system.

	Generation cost ($/h)	Damping ratio (%)	Critical eigenvalue
BCO	51384	−12.2	0.301 ± 2.429i
SSO	51761 —	Stability boundary Positive DR	0 Failed
PSM	51674 52308	Stability boundary 3	0 −0.225 ± 7.560i

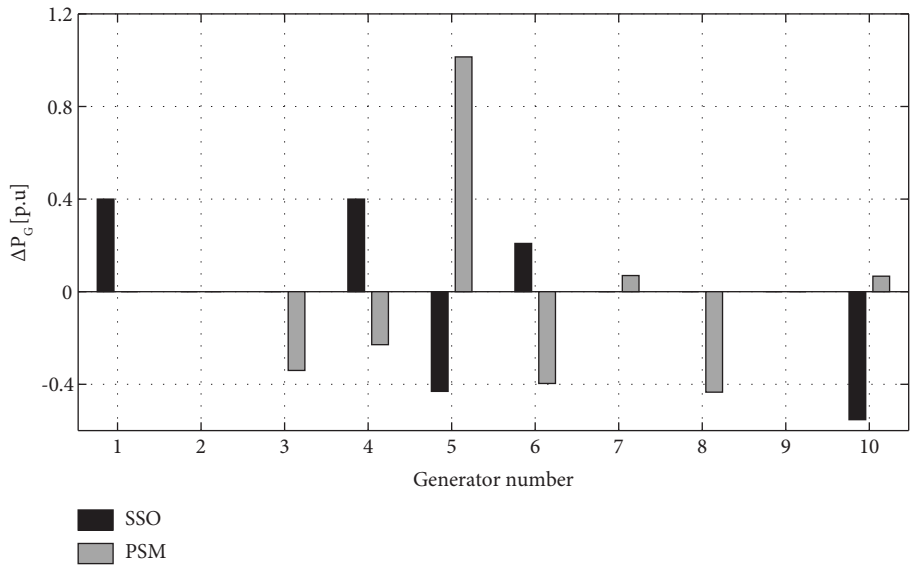

Figure 10: Generation redispatch to reach the stability boundary for IEEE 39-bus system.

buses 8 and 9). In this case, the system has a critical mode as $0.301 \pm 2.429i$. Table 3 presents simulation results for different methods.

Based on simulation results, the proposed method provides a lower-cost stability boundary than the SSO method. Changes in the output power of generators to reach

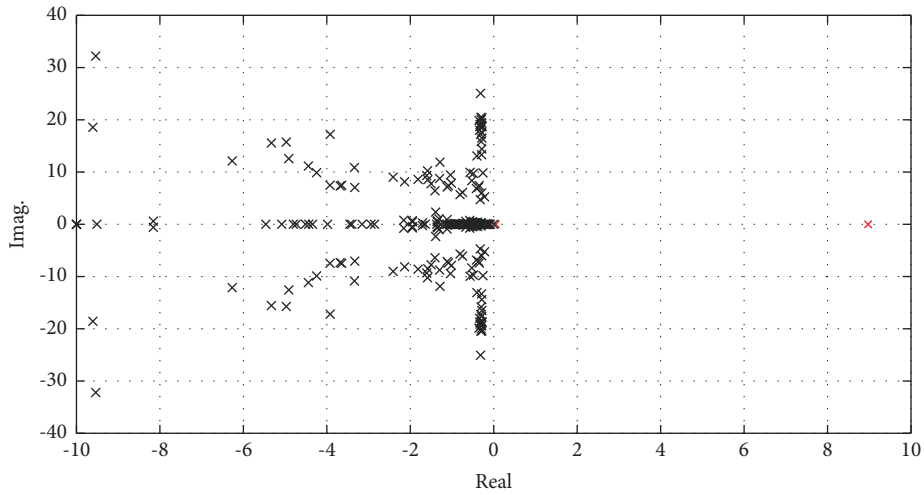

Figure 11: Eigenvalues in the basic operating point for IEEE 118-bus system.

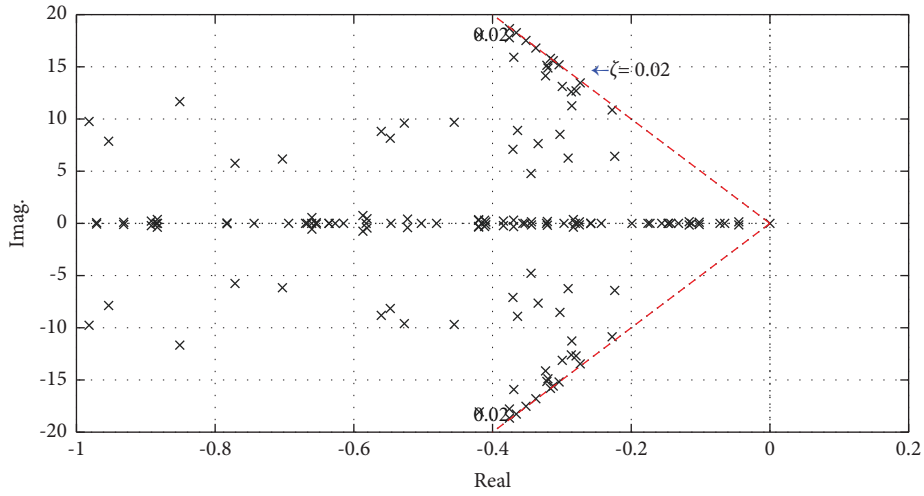

Figure 12: Eigenvalues after applying the proposed method for IEEE 118-bus system.

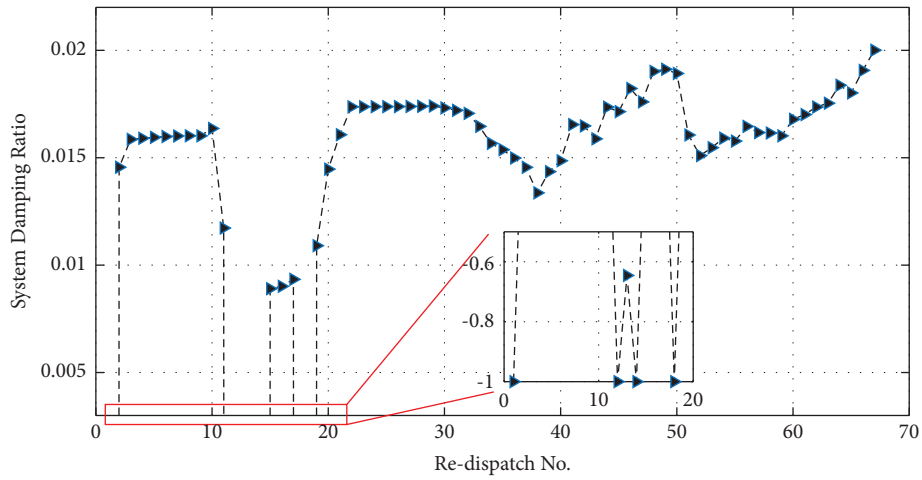

Figure 13: Trace of system damping ratio for IEEE 118-bus system.

the stability boundary are shown in Figure 10. It should be noted that the proposed method can increase the damping of the system to a desirable level (3%).

4.3. IEEE 118-Bus System. The IEEE 118-bus system has 54 generators, and the steady-state and dynamic data of this system are taken from [28, 32], respectively. Based on small signal stability analysis at the base operating point, the presence of positive modes has caused the system to become unstable. The system eigenvalues in the base operating point are shown in Figure 11.

Considering these conditions, the proposed method is used to stabilize the system providing an appropriate damping ratio. For this system, a damping ratio of 2% is considered. Figure 12 shows the eigenvalues of the system after implementing the proposed method. It is clear that the system has successfully moved out of the unstable region, and proper damping has been provided. Furthermore, the path of the minimum damping ratio of the system is shown in Figure 13, which shows that the trend of enhancing system damping is not uniform.

5. Conclusion

The generation rescheduling algorithm proposed in this article provides a scheme to redispatch the active output power of the generators to ensure the small signal stability and enhance the minimum damping ratio of the power system. The stabilization process is performed sequentially by solving the optimization problem and small signal stability analysis until a desired area of operation is reached. Considering the sequential nature of the proposed method, it is well suited to addressing the problem of changing the critical eigenvalues of the system by changing the operating conditions as well as allowing the operator to select its desired operating point from a set of operating points.

A second-order convex redispatch model was used instead of the AC optimal power flow to make the proposed method computationally tractable to effectively compute the optimization direction, the system generators and system buses are divided into two increasing and decreasing groups using modal and sensitivity analysis. The simulation of the proposed method on three IEEE test systems verifies the effectiveness of the proposed sequential method to ensure small signal stability. Two systems are stable at the base operating point, and the proposed method increases the system's damping to the desired level. The third system is unstable; after it stabilizes, appropriate damping is produced. The impact of other tools to improve the small signal stability were not addressed in this paper and can be investigated in future works.

Appendix

This appendix presents the differential and algebraic equations of the power system.

(1) Synchronous machine and exciter differential equations:

$$\begin{aligned}
\frac{\mathrm{d}\delta_i}{\mathrm{d}t} &= \omega_i - \omega_s,\\
\frac{\mathrm{d}\omega_i}{\mathrm{d}t} &= \frac{T_{Mi}}{M_i} - \frac{\left[E'_{qi} - X'_{di}I_{di}\right]I_{qi}}{M_i} - \frac{\left[E'_{di} - X'_{qi}I_{qi}\right]I_{di}}{M_i},\\
\frac{\mathrm{d}E'_{qi}}{\mathrm{d}t} &= -\frac{E'_{qi}}{T'_{doi}} - \frac{(X_{di} - X'_{di})I_{di}}{T'_{doi}} + \frac{E_{fdi}}{T'_{doi}},\\
\frac{\mathrm{d}E'_{di}}{\mathrm{d}t} &= -\frac{E'_{di}}{T'_{qoi}} - \frac{\left(X_{qi} - X'_{qi}\right)I_{qi}}{T'_{qoi}},\\
\frac{\mathrm{d}E_{fdi}}{\mathrm{d}t} &= -\frac{K_{Ei} + S_E\left(E_{fdi}\right)}{T_{Ei}}E_{fdi} + \frac{V_{Ri}}{T_{Ei}},\\
S_E\left(E_{fdi}\right) &= A_{ei}e^{B_{ei}E_{fdi}},\\
\frac{\mathrm{d}V_{Ri}}{\mathrm{d}t} &= -\frac{V_{Ri}}{T_{Ai}} + \frac{K_{Ai}}{T_{Ai}}R_{fi} - \frac{K_{Ai}K_{Fi}}{T_{Ai}T_{Fi}}E_{fdi} + \frac{K_{Ai}}{T_{Ai}}\left(V_{refi} - V_i\right),\\
\frac{\mathrm{d}R_{Fi}}{\mathrm{d}t} &= -\frac{R_{Fi}}{T_{Fi}} + \frac{K_{Fi}}{(T_{Fi})^2}E_{fdi}, \quad (\text{for} \quad i \in \mathbb{N}_G).
\end{aligned} \tag{A1}$$

(2) Stator algebraic equations:

$$\begin{aligned}
&E'_{di} - V_i\sin\left(\delta_i - \theta_i\right) - R_{si}I_{di} + X'_{qi}I_{qi} = 0,\\
&E'_{qi} - V_i cos\left(\delta_i - \theta_i\right) - R_{si}I_{qi} - X'_{di}I_{di} = 0 \quad (\text{for } i \in \mathbb{N}_G).
\end{aligned} \tag{A2}$$

(3) Network algebraic equations:

$$\begin{aligned}
&I_{di}V_i\sin\left(\delta_i - \theta_i\right) + I_{qi}V_i\cos\left(\delta_i - \theta_i\right) + P_{Li}\left(V_i\right)\\
&\quad - \sum_{k\in\mathbb{N}_B} V_iV_kY_{ik}\cos\left(\theta_i - \theta_k - \alpha_{ik}\right) = 0,\\
&I_{di}V_i\cos\left(\delta_i - \theta_i\right) - I_{qi}V_i\sin\left(\delta_i - \theta_i\right) + Q_{Li}\left(V_i\right)\\
&\quad - \sum_{k\in\mathbb{N}_B} V_iV_kY_{ik}\sin\left(\theta_i - \theta_k - \alpha_{ik}\right) = 0, \quad (\text{for } i \in \mathbb{N}_G),\\
&P_{Lj}\left(V_j\right) - \sum_{k\in\mathbb{N}_B} V_jV_kY_{jk}\cos\left(\theta_j - \theta_k - \alpha_{jk}\right) = 0,\\
&Q_{Lj}\left(V_j\right) - \sum_{k\in\mathbb{N}_B} V_jV_kY_{jk}\sin\left(\theta_j - \theta_k - \alpha_{jk}\right) = 0, \quad (\text{for } j \in \mathbb{N}_{PQ}).
\end{aligned} \tag{A3}$$

Nomenclature

Indices

i: Index of generators
k, j: Indices of buses
$\mathbb{N}_B$: Set of system buses
$\mathbb{N}_G$: Set of generator buses
$\mathbb{N}_{PQ}$: Set of PQ buses

Parameters

ω_s: Rated rotor speed
X_{di}/X_{qi}: d-axis/ q-axis components of the synchronous reactance of i^{th} generator

X'_{di}/X'_{qi}: d-axis/ q-axis components of the transient reactance of i^{th} generator
T'_{d0i}/T'_{q0i}: d-axis/ q-axis components of the open-circuit time constant of i^{th} generator
T_{Mi}: Mechanical torque of i^{th} generator
M_i: Inertia constant of i^{th} generator
D_i: Damping torque coefficient of i^{th} generator
R_{si}: Winding resistance of i^{th} generator
$S_E(E_{f\ di})$: Field saturation function
$K_{Ei}/K_{Ai}/K_{Fi}$: Exciter/voltage regulator/feedback gain of i^{th} generator
$T_{Ei}/T_{Ai}/T_{Fi}$: Exciter/voltage regulator/feedback time constant of i^{th} generator
$V_{\text{ref}k}$: Reference voltage of k^{th} bus
P_{Lk}/Q_{Lk}: Active and reactive load of k^{th} bus
Y_{jk}/ϕ_{jk}: Magnitude/phase angle of the admittance matrix

Variables

δ_i: Rotor angle of i^{th} generator
ω_i: Rotor speed of i^{th} generator
E'_{di}/E'_{qi}: d-axis/q-axis components of the internal voltage of i^{th} generator
E_{fdi}: Excitation output voltage of i^{th} generator
V_{Ri}: Voltage regulator output of i^{th} generator
R_{Fi}: Exciter rate feedback of i^{th} generator
I_{di}/I_{qi}: d-axis/ q-axis components of the internal current of i^{th} generator
V_k/θ_k: Voltage magnitude/phase angle of k^{th} bus.

Data Availability

The numerical data used to support the findings of this study are included within the article.

Conflicts of Interest

The authors declare that there are no conflicts of interest regarding the publication of this article.

References

[1] D. D. Simfukwe, B. C. Pal, N. Martins, and R. Jabr, "Robust and low-order design of flexible ac transmission systems and power system stabilisers for oscillation damping," *IET Generation, Transmission and Distribution*, vol. 6, no. 5, pp. 445–452, 2012.

[2] M. Eslami, H. Shareef, A. Mohamed, and M. Khajehzadeh, "Coordinated design of pss and svc damping controller using cpso," in *Proceedings of the 2011 5th International Power Engineering and Optimization Conference*, pp. 11–16, IEEE, Shah Alam, Malaysia, June 2011.

[3] M. Khosravi-Charmi and T. Amraee, "Wide area damping of electromechanical low frequency oscillations using phasor measurement data," *International Journal of Electrical Power and Energy Systems*, vol. 99, pp. 183–191, 2018.

[4] M. Eslami, H. Shareef, A. Mohamed, and M. Khajehzadeh, "Damping controller design for power system oscillations using hybrid GA-SQP," *International Review of Economics Education*, vol. 6, no. 2, pp. 888–896, 2011.

[5] M. Eslami, H. Shareef, A. Mohamed, and M. Khajehzadeh, "Optimal location of PSS using improved PSO with chaotic sequence," in *Proceedings of the International Conference on Electrical, Control and Computer Engineering 2011 (InECCE)*, pp. 253–258, IEEE, Shah Alam, Malaysia, June 2011.

[6] L. Zeng, W. Yao, Q. Zeng et al., "Design and real-time implementation of data-driven adaptive wide-area damping controller for back-to-back VSC-HVDC," *International Journal of Electrical Power and Energy Systems*, vol. 109, pp. 558–574, 2019.

[7] C. Y. Chung, L. Wang, F. Howell, and P. Kundur, "Generation rescheduling methods to improve power transfer capability constrained by small-signal stability," *IEEE Transactions on Power Systems*, vol. 19, no. 1, pp. 524–530, 2004.

[8] Y. Xu, Z. Y. Dong, R. Zhang, and K. Po Wong, "A decision tree-based on-line preventive control strategy for power system transient instability prevention," *International Journal of Systems Science*, vol. 45, no. 2, pp. 176–186, 2014.

[9] F. Thams, L. Halilbasic, P. Pinson, S. Chatzivasileiadis, and R. Eriksson, "Data-driven security-constrained opf," *In Proc. 10th Bulk Power Syst. Dyn. Control Symp*, vol. 1, pp. 1–10, 2017.

[10] L. Halilbašić, F. Thams, A. Venzke, S. Chatzivasileiadis, and P. Pinson, "Data-driven security-constrained AC-OPF for operations and markets," in *Proceedings of the 2018 Power Systems Computation Conference (PSCC)*, pp. 1–7, IEEE, Dublin, Ireland, June 2018.

[11] A. V. Murzakhanov, G. S. Misyris, and S. Chatzivasileiadis, "Neural networks for encoding dynamic security-constrained optimal power flow," 2021, https://arxiv.org/abs/2003.07939.

[12] L. Wang, D. Yang, G. Cai, H. Gao, and Z. Chen, "Synchronized-ambient-data-driven participation-factor-based generation rescheduling strategy for enhancing the damping level of interconnected power systems," *International Journal of Electrical Power and Energy Systems*, vol. 146, Article ID 108740, 2023.

[13] R. Zárate-Miñano, F. Milano, and A. J. Conejo, "An OPF methodology to ensure small-signal stability," *IEEE Transactions on Power Systems*, vol. 26, no. 3, pp. 1050–1061, 2011.

[14] F. Alvarado, C. DeMarco, I. Dobson, and P Sauer, "Avoiding and suppressing oscillations," *PSERC project final report*, vol. 1, 1999.

[15] H. K. Nam, Y. K. Kim, K. S. Shim, and K. Y. Lee, "A new eigen-sensitivity theory of augmented matrix and its applications to power system stability analysis," *IEEE Transactions on Power Systems*, vol. 15, no. 1, pp. 363–369, 2000.

[16] J. Condren and T. W. Gedra, "Expected-security-cost optimal power flow with small-signal stability constraints," *IEEE Transactions on Power Systems*, vol. 21, no. 4, pp. 1736–1743, 2006.

[17] P. Li, H. Wei, B. Li, and Y. Yang, "Eigenvalue optimisation based optimal power flow with small signal stability constraints," *IET Generation, Transmission and Distribution*, vol. 7, no. 5, pp. 440–450, 2013.

[18] M. M. Othman and S. Busan, "A novel approach of rescheduling the critical generators for a new available transfer capability determination," *IEEE Transactions on Power Systems*, vol. 31, no. 1, pp. 3–17, 2016.

[19] C. Li, H. D. Chiang, and Z. Du, "Network-preserving sensitivity-based generation rescheduling for suppressing power system oscillations," *IEEE Transactions on Power Systems*, vol. 32, no. 5, pp. 3824–3832, 2017.

[20] T. J. Parreiras, S. Gomes Jr, G. N. Taranto, and K. Uhlen, "Closest security boundary for improving oscillation damping through generation redispatch using eigenvalue sensitivities," *Electric Power Systems Research*, vol. 160, pp. 119–127, 2018 Jul 1.

[21] P. Pareek and H. D. Nguyen, "A convexification approach for small-signal stability constrained optimal power flow," *IEEE Transactions on Control of Network Systems*, vol. 8, no. 4, pp. 1930–1941, 2021 Jun 23.
[22] M. K. Singh and V. Kekatos, "Optimal power flow schedules with reduced low-frequency oscillations," 2022, https://arxiv.org/abs/2204.08998.
[23] P. Li, J. Qi, J. Wang, H. Wei, X. Bai, and F. Qiu, "An SQP method combined with gradient sampling for small-signal stability constrained OPF," *IEEE Transactions on Power Systems*, vol. 32, no. 3, pp. 2372–2381, 2017.
[24] Y. Li, G. Geng, Q. Jiang, W. Li, and X. Shi, "A sequential approach for small signal stability enhancement with optimizing generation cost," *IEEE Transactions on Power Systems*, vol. 34, no. 6, pp. 4828–4836, 2019.
[25] A. J. Wood, B. F. Wollenberg, and G. B. Sheblé, *Power Generation, Operation, and Control*, John Wiley and Sons, Hoboken, NJ, USA, 2013.
[26] P. S. Kundur and O. P. Malik, *Power System Stability and Control*, McGraw-Hill Education, New York, NY, USA, 2022.
[27] P. W. Sauer and M. A. Pai, *Power System Dynamics and Stability*, Prentice-Hall, Hoboken, NJ, USA, 1998.
[28] A. Pizano-Martínez, C. R. Fuerte-Esquivel, E. A. Zamora-Cárdenas, and J. M. Lozano-García, "Directional derivative-based transient stability-constrained optimal power flow," *IEEE Transactions on Power Systems*, vol. 32, no. 5, pp. 3415–3426, 2017.
[29] R. D. Zimmerman, C. E. Murillo-Sánchez, and R. J. Thomas, "MATPOWER: steady-state operations, planning, and analysis tools for power systems research and education," *IEEE Transactions on Power Systems*, vol. 26, no. 1, pp. 12–19, 2011.
[30] P. M. Anderson and A. A. Fouad, *Power System Control and Stability*, John Wiley and Sons, Hoboken, NJ, USA, 2008.
[31] M. A. Pai, *Energy Function Analysis for Power System Stability*, Kluwer Academic Publishers, Boston, MA, London, 1989.
[32] Dynamic IEEE Test Systems, 2022, https://www.kios.ucy.ac.cy/testsystems/index.php/ieee-118-bus-modified-test-system/.